NASA TECHNICAL MEMORANDUM

NASA TM-75328

PRACTICAL CALCULATION OF LAMINAR AND TURBULENT BLED-OFF BOUNDARY LAYERS

R. Eppler

Translation of "Praktische Berechnung laminarer und
turbulenter Absauge-Grenzschichten," Ingenieur-
Archiv, Vol. 32, No. 4, 1963, pp. 221-245

NATIONAL AERONAUTICS AND SPACE ADMINISTRATION
WASHINGTON, D.C. 20546 SEPTEMBER 1978

1. Report No. NASA TM-75328	2. Government Accession No.	3. Recipient's Catalog No.
4. Title and Subtitle PRACTICAL CALCULATION OF LAMINAR AND TURBULENT BLED-OFF BOUNDARY LAYERS		5. Report Date September 1978
		6. Performing Organization Code
7. Author(s) R. Eppler Bölkow-Entwicklungen KG		8. Performing Organization Report No.
		10. Work Unit No.
9. Performing Organization Name and Address Leo Kanner Associates Redwood City, California 94063		11. Contract or Grant No. NASw-3199
		13. Type of Report and Period Covered Translation
12. Sponsoring Agency Name and Address National Aeronautics and Space Administration, Washington, D.C. 20546		
		14. Sponsoring Agency Code

15. Supplementary Notes

Translation of "Praktische Berechnung laminarer und turbulenter Absauge-Grenzschichten", Ingenieur-Archiv, Vol. 32, No. 4, 1963, pp. 221 -245 .

16. Abstract

17. Key Words (Selected by Author(s))		18. Distribution Statement Unclassified-Unlimited

19. Security Classif. (of this report) Unclassified	20. Security Classif. (of this page) Unclassified	21. No. of Pages	22. Price

PRACTICAL CALCULATION OF LAMINAR AND TURBULENT BLED-OFF BOUNDARY LAYERS[1]

R. Eppler
Bölkow-Entwicklungen KG

1.   Introduction

Bleed-off of boundary layer material through small ori-
fices or porosities at the wall in contact with flow has long
been known as effective means for improvement of flow character-
istics [1]. On the one hand it permits longer conservation of
the laminar boundary layer and on the other it helps prevent
separation of the turbulent boundary layer, or retards it [2],
both of which can lead to considerable reductions of drag.
Often the two effects of bleed-off overlap. Where bleed off
is present in an air foil, for preservation of laminarity at
high-speed flight, it will also have a certain effect in re-
tarding the separation when it can no longer prevent the
reversal during slow flight. Conversely, continuous siphoning
for lift increase, i.e., for retardation of separation during
slow flight, must in principle have a favorable influence on
the reversal at high-speed flight during a change in pressure
distribution. Up til now hardly any thought has been given to
the combination of these two effects, since entirely different
amounts of bleed-off are required at different points. But
lately there has been some approach to this combination. A
valuable aid in realizing such a bleed-off combination is a
method of calculation that permits uniform treatment of all
cases.

---

*Numbers in the margin indicate pagination in the foreign text.

This study will report on a solution of the problem. In the foreground will be the method of calculation with one parameter by means of Kármán's [3] Conservation of Momentum and of Wieghardt's [4] energy theorem, which was first applied successfully by A. Walz for laminar boundary layers [5]. Since then the method has proven itself for many other purposes. Wieghardt [6] calculated laminar boundary layers with bleed-off in which the minimum amount of suction needed for conservation of laminar flow was also calculated. Truckenbrodt [7] extended Walz's method to turbulent boundary layers by using semiempirical equations based on experimental and theoretical investigations by Ludwieg and Tillmann [8], and Rotta [9], instead of different relations derived from velocity profiles during laminar flow. The mathematical simplifications used did result in unattractive errors for a few special cases, particularly in the vicinity of the turbulent separation point. Schulz [10] offered an improvement, particularly effective for that point. A procedure by Walz []]] for the turbulent case including compressibility, which operates without mathematical simplifications, is semigraphical and thus little suited for the digital computer. Only lately have Schlichting and Pechau [12,13] reported on the extension of Truckenbrodt's theory of turbulence to bleed-off, in which additional mathematical simplifications were carried out. Such simplifications are particularly annoying since the empirical fundamentals of the theory of turbulence are still uncertain. It is hard to distinguish whether existing shortcomings are of purely mathematical nature or if they are due to the empirical fundamentals.

For a case without bleed-off it was recently tried to avoid the simplifications introduced by Truckenbrodt; this led, simultaneously, to further unification of laminar and turbulent cases and a possibility for simple programming on digital computers [14]. It was demonstrated that the empirical

2

fundamentals used by Truckenbrodt are better than the results
gained with the method had led one to suspect. Extension of
those methods to the case of bleed-off, which will be presented
subsequently, again permits simultaneous treatment of laminar
and turbulent boundary layers and solves the approximation dif-
ferential equations, according to the best presently available
empirical fundamentals, without an uncertain error. Here, too,
a big difference is shown from Schlichting and Pechau. Unfor-
tunately, possibilities for comparison of experiments are still
sparse. But the results gained are entirely plausible and
because a large amount can be obtained in a simple way, and
quickly, it has become possible to check any and all experi-
mental results with them. Differences between theory and ex-
periment can be pursued back to the empirical fundamentals
because of the easily grasped method of solution, permitting
their verification and correction.

The case without bleed-off, which is completely contained
as special case, will be treated in detail once more, since my
cited lecture appeared in print without the corresponding illus-
trations.

2.   Basic Equations

The following quite well known relations (with subse-
quently explained symbols) can be formed from L. Prandtl's
well known partial differential equations for velocity $u(x,y)$
in the boundary layer (see Fig. 1), by formation of moments
through application of Bernoulli's equation for the outside
flow $U(x)$ in the plane incompressible case, according to von
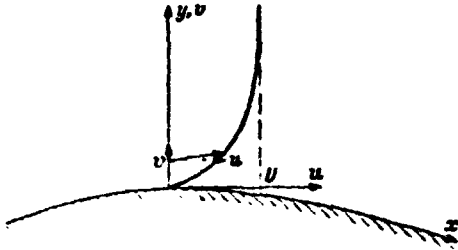Kármán and Wieghardt:

3

Fig. 1 Sketch of Coordinates and Velocities.

$$\frac{1}{U^2}\frac{d}{dx}(U^2\delta_2) + \frac{\delta_1}{U}\frac{dU}{dx} = \frac{\tau_0}{\varrho U^2} + \frac{v_0}{U}, \tag{1}$$

$$\frac{1}{U^3}\frac{d}{dx}(U^3\delta_3) = 2\frac{d+l}{\varrho U^3} + \frac{v_0}{U}. \tag{2}$$

where v_0 is normal velocity at the wall, positive in the y-direction (blow-off). According to Walz [5] displacement thickness is shown as

$$\delta_1(x) = \int_0^\infty \left(1 - \frac{u(x,y)}{U(x)}\right)dy \tag{3}$$

the so-called pulse and energy loss thickness as

$$\delta_2 = \int_0^\infty \frac{u}{U}\left(1 - \frac{u}{U}\right)dy \tag{4}$$

and

$$\delta_3 = \int_0^\infty \frac{u}{U}\left[1 - \left(\frac{u}{U}\right)^2\right]dy. \tag{5}$$

Symbol τ_0, which occurs in the Conservation of Momentum equation (1), is shearing stress at the wall

$$\tau_0 = \varrho \nu \left(\frac{\partial u}{\partial y}\right)_0 \tag{6}$$

in

$$\frac{d+l}{\varrho U^2} = \int_0^\infty \frac{\tau}{\varrho U^2}\frac{\partial}{\partial y}\left(\frac{u}{U}\right)dy \tag{7}$$

4

from equation (2), generated at first formally during formation
of moments, in which d is interpreted as energy dissipation and
t as change in turbulence (disappearing for laminar flow). The
whole equation (2) can be treated as energy theorem. The (con-
stant) density of the flowing medium is ρ, kinematic viscosity
is ν.

Shearing stress τ from equation (7) is analogous to (6)
for laminar flow

$$\tau = \rho \nu \frac{\partial u}{\partial y}.$$ (8)

but still represents a big uncertainty for the turbulent boun-
dary layer.

Equations (1) and (2) are at first valid only for the as-
sumption that the solution u(x,y) of the partial Prandtl dif-
ferential equation is known for the given functions of U(x)
and v_0(x) and that the values required for equations (1) and
(2) can be calculated from (3) to (7) with it. For the case
of turbulent flow velocities averaged over time can be used
during consideration of the contribution of turbulence to
shearing stress.

Reversal of the calculation procedure for an approximate
solution is carried out by making certain assumptions about the
distribution u(x,y), and for the case of turbulent flow also
about shearing stress τ. This will be described in more detail
in the following section.

3.   Form Parameter, Wall Shearing Stress and Dissipation for
      Turbulent Flow

Two relations, (1) and (2), are available for δ_i. A
statement can be made for u(x,y), which contains two independent

values. Usually one independent value is taken for the thickness of the boundary layer, that is for distortion of u(x,y) in the y-direction, another for the shape of the boundary layer through a statement like

$$\frac{u(x,y)}{U(x)} = f\left[\lambda(x) \cdot \frac{y}{\delta(x)}\right]. \tag{9}$$

by entering this arrangement into (3) to (8) one gets all the values defined by (3) to (7) as functions of $\delta(x)$ and $\lambda(x)$; equations (1) and (2) become a system of differential equations for these two unknown values. Approximations can be obtained subsequently with their solutions, for u(x,y) from equation (9), for the δ_i from (3) to (5).

There is a large number of different equations (9) and many methods and procedures for their solutions. The following one, introduced by Walz and Wieghardt, appears to be the most easily understood calculation method. When entering (9) in (3) the transformation $\eta = y/\delta$ shows that δ_1 is proportional to δ, i.e., that δ_1/δ depends on λ only because

$$\delta_1 = \int_0^\infty [1 - f(\lambda, \eta)] \, \delta \, d\eta \tag{10}$$

The same holds for δ_2 and δ_3. This makes the quotient of two δ_i a function of λ only, which can be obtained once and for all for each given (9). For instance, by putting

$$\frac{\delta_3}{\delta_2} = H_{32} \tag{11}$$

and

$$\frac{\delta_1}{\delta_2} = H_{12} \tag{12}$$

6

$H_{12}=F(H_{32})$ can be obtained by elimination of λ and δ_1, which is needed in equation (1), expressed in δ_2 and δ_3. Should one succeed in expressing shearing stress and dissipation similarly simply through δ_2 and δ_3, the solution of the (1) and (2) equation system is recommended without further transformation. According to (6) and (9) shearing stress at the wall is

$$\frac{\tau_0}{\rho\ U^2} = \frac{\nu}{U\delta_2}\frac{\partial f}{\partial \eta}\Big|_0 = \frac{\nu}{U\delta_2}\ \varepsilon^*(H_{32}). \tag{13}$$

Here is δ_2/δ_i, already shown as function of λ only; this can also be arranged for $\partial f/\partial \eta$ through (9). Through reversal of (11) shearing stress at the wall can also be expressed through δ_2 and δ_3.

Dissipation can also be brought into suitable form through

$$\frac{d+t}{\rho\ U^3} = \frac{\nu}{U\delta_2}\delta \int_0^\infty \left(\frac{\partial f}{\partial \eta}\right)^2 d\eta = \frac{\nu}{U\delta_2}\ D^*(H_{32}) \tag{14}$$

As soon as the functions $H_{32}(\lambda)$, $H_{12}(H_{32})$, $\varepsilon^*(H_{32})$ and $D^*(H_{32})$ have been obtained for a given equation (9) the system (1) and (2) must be integrated numerically. With the results $\delta_2(x)$ and $\delta_\varepsilon(x)$ one can find H_{32}, from it λ and, with the aid of equation (9), the basic velocity distribution $u(x,y)$. In most cases the last step is not carried out; generally it is quite satisfactory to have in δ_2 a value for friction losses and in λ [or equivalent value, like H_{32} from (11)] an indication for the shape, resp. the separation tendency of the boundary layer.

Everything has not been traced back to equation (9). The closer on. comes to the exact solution $u(x,y)$ with it the better

7

will be the results. The most important boundary conditions are, therefore, fulfilled in advance in function $f(\lambda, y/\delta)$ from equation (9)

$$f(\lambda,0) = 0, \quad f(\lambda,\infty) = 1, \quad \frac{f}{y}\bigg|_{\lambda\infty} = 0 \qquad (15)$$

It is already sufficient to fulfill the last two boundary conditions in the finite, i.e., for the distance of a certain boundary layer thickness δ from the wall, or $\eta=1$. Even though Walz has shown that after consideration of (15) the special equation (9) has little influence on results where no bleed-off occurs, some attention will still be devoted to that question since the joint treatment of bled off boundary layers and uninfluenced ones includes a large range of various velocity profiles, which could create inaccuracies. Important is only the influence on the three functions required for (1) and (2).

A particularly good premise was already provided by Pohlhausen (15). He puts

$$\frac{u}{U} = P_1(\eta) + \lambda(x)\, P_2(\eta) \quad \text{for} \quad n \leqq 1,$$

$$\frac{u}{U} = 1 \qquad\qquad\qquad \text{for} \quad n > 1$$

and fulfills the boundary conditions with the fourth degree polynomials P_1 and P_2 (equation (15)). This so-called P_4-statement is, like the improved P_6-statement, too coarse for our purposes. Much better suitable are surely the velocity profiles that are generated at the so-called "similar boundary layers" (Hartree profile), particularly for flows where the form parameter does not vary quickly. Walz [5] already employed these solutions, which are exact for certain velocity distributions, for calculation of the required connections.

8

Inaccuracies that have slipped in do not play an important role in Walz's case but they carry more weight in the calculation of bleed-off conditions. For that reason a few more similar solutions were obtained with the corresponding values for H_{32}, H_{12}, ϵ^* and D^* (Hartree profile). In Fig. 2 data points are plotted for the similar solutions without bleed-off for increasing pressure (Hartree profile) and others for solutions of the flat plate with bleed off. In addition a data point is plotted for $H_{32}=5/3$, which was obtained from the so-called asymptotic solution of the plate with constant bleed-off. The following approximation was chosen for the calculation to provide good approximation for the entire range:

a. Values obtained from the Hartree profiles were approximated for the range $1.51509 \leq H_{32} \leq 1.57258$, which corresponds to the pressure increase range between the flat plate and separation for Hartree profiles. $H_{32}=1.51509$ is, therefore, the separation boundary.

b. In place of the Hartree profiles of pressure decrease the similar bleed-off profiles of the plate were used, complemented by the point of asymptotic bleed off.

Boundary layers free of bleed-off are characterized somewhat less accurately that way. But in this case accuracy is of less importance.
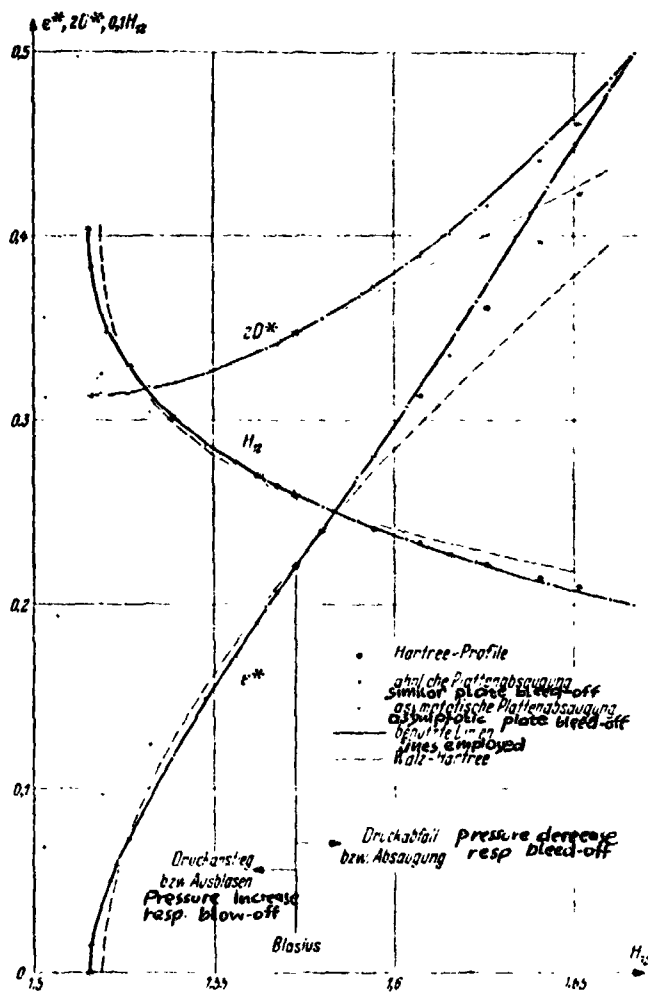
The approximations

$$
\begin{aligned}
H_{12} &= 4{,}02922 - (583{,}60182 - 724{,}55916\,H_{32} + 227{,}18220\,H_{32}^2) \mid H_{32} - 1{,}51509 \mid \\
&\qquad \text{for} \quad 1{,}51509 < H_{32} < 1{,}57258, \\
H_{12} &= 79{,}870845 - 89{,}582142\,H_{32} + 25{,}715786\,H_{32}^2 \\
&\qquad \text{for} \quad H_{32} > 1{,}57258,
\end{aligned}
\qquad (16)
$$

9

$$\varepsilon^* = 2{,}512589 - 1{,}686095\,H_{12} + 0{,}391541\,H_{12}^2 - 0{,}031720\,H_{12}^3$$
$$\text{für} \qquad 1{,}51509 \leqq H_{32} \leqq 1{,}57258\,,$$
$$\varepsilon^* = 1{,}372391 - 4{,}226253\,H_{32} + 2{,}221687\,H_{32}^2$$
$$\text{für} \qquad H_{32} > 1{,}57258\,, \tag{17}$$

$$D^* = 7{,}853976 - 10{,}260551\,H_{32} + 3{,}418898\,H_{32}^2 \tag{18}$$

Fig. 2   The General Boundary Layer-Functions $H_{12}(H_{32})$, $\varepsilon^*(H_{32})$ and $D^*(H_{32})$ in Several Directions.

10

are suitable for generation of computer programs. The dif-
ference between these approximation functions and the approxi-
mated values is smaller by an order of magnitude than the dif-
ference between the various boundary layer profiles being dis-
cussed. For calculations by hand it is best to use accurate
diagrams of the functions (16) to (:), which are easily ob-
tained with Table I.

The choice made provides very good coverage of similar   /226
solutions without bleed-off with pressure increase to the flat
plate (Blasius Flow), as well as for similar bleed-off boundary
layers of the flat plate. All other calculations of boundary
layers with the present method contain an error brought about
purely by the procedure, which will be explained with several
examples.

Table I

Values of Laminar Boundary Layer Functions
$H_{12}(H_{32})$, $\epsilon^*(H_{32})$ and $D^*(H_{32})$

H_{32}	H_{12}	ϵ^*	D^*
1.51509	4.02922	0.00000	0.15638
1.51575	3.83366	0.01167	0.15639
1.52099	3.48079	0.04911	0.15672
1.52630	3.29673	0.07303	0.15741
1.53863	3.02095	0.11796	0.16006
1.54803	2.87178	0.14828	0.16292
1.55568	2.77120	0.17166	0.16571
1.56214	2.69668	0.19071	0.16841
1.56771	2.63838	0.20674	0.17100
1.57258	2.59110	0.22052	0.17340
1.60353	2.34611	0.30706	0.19219
1.62256	2.22429	0.36408	0.20808
1.64289	2.11182	0.42685	0.22559
1.66020	2.02846	0.48039	0.24313
1.66667	2.00000	0.50000	0.25000

11

4. Form Parameters, Wall Shearing Stress and Dissipation for Turbulent Flow

Since the laminar boundary layer is easily handled, according to the results in section 3, a corresponding path will be followed for solutions of the turbulent layer. The only significant difference will be that shearing stress can no longer be expressed through equation (8) in the turbulent boundary layer. As function of the turbulent motions of variation and the energy transport connected with it additional "apparent" shearing stresses occur at first, which call for other relations in place of (8). In addition, the velocity profiles take on completely different forms so that statement (9) does no longer cover them completely and energy dissipation cannot be obtained the same way as before. But wall shearing stress (6) is not influenced since no turbulence is possible and effective in close proximity to the wall.

So far it has not been possible to get useful results for the theory of turbulent boundary layers based only on laws about the turbulent shearing stress together with velocity statements. But just as we could liberate ourselves, with the aid of general functions from the velocity profile, of the boundary layer in the laminar case so will relations which permit calculation of wall shearing stress and energy dissipation from the independent variables, δ_2 and δ_3, also suffice in the turbulent case. Such relations for the wall shearing stress were stated by Ludwieg and Tillmann [8] as

$$\frac{\tau_0}{\rho U^2} = 0.123 \left(\frac{U \delta_2}{\nu} \right)^{-0.268} 10^{-0.678 H_{12}} \tag{19}$$

for dissipation by Rotta [9]. Rotta's results were used by Truckenbrodt [7] in simplified form

12

$$\frac{d+i}{\rho U^2} = 0.0056\left(\frac{U\delta}{v}\right)^{-\frac{1}{6}}$$

(20)

which has proven itself well for the case without bleed-off [1]
like the connection of form parameters based on Wieghardt [16]

$$H_{32} = \frac{0.379\, H_{32}}{H_{32} - 1.269}$$

(21)

The validity range for equations (19) to (21) must be ex- /227
plained in more detail since for the case of bleed-off larger
form parameter ranges will again overlap. At first (19) was
obtained for values of H_{12} between 1.2 and 2.4, corresponding
to H_{12} values between 1.5 and 1.85 per equation (21). Equa-
tion (20) also is valid in the same range. No overlap in
range will be of concern for the pressure increase up to sep-
aration, which occurs at about $H_{32}=1.5$. But a strong tendency
to high H_{32} values is present for the range of pressure de-
crease or for bleed-off. Pechau [3] has given examples where
H_{32} values from 3 to 5 were reached. The range of high H_{32}
values or low H_{12} values must, therefore, be observed sepa-
rately.

A possibility for extrapolation from the Ludwieg-Tillmann
law is offered by the following boundary consideration. After
δ_2 and δ_3 are defined by equations (4) and (5) one gets

$$\delta_3 = \int_0^\infty \frac{u}{U}\left(1 - \frac{u}{U}\right)\left(1 + \frac{u}{U}\right)dy < 2\delta_2,$$

(22)

13

as long as u<U, since the second parenthesis can be maximized
with the value of 2. As long as there are no excess velocities
present in the boundary layer, which is not to be expected
without tangential blow-off,

$$H_{32} < 2 \tag{23}$$

according to statement (11). Based on the same assumption
$H_{12} > 1$ from comparison of (3) and (4). The nature of boundary
layer profiles leading to H_{32} values near 2 is also easily
grasped. For instance, if one wants to reach

$$H_{32} > 2 - \varepsilon \tag{24}$$

then for $1 - u/U = \bar{u}$ in statement (5),

$$\delta_3 = \int_0^\infty (1-\bar{u})\bar{u}(2-\bar{u})\,dy > (2-\varepsilon)\delta_2 \tag{25}$$

so

$$\int_0^\infty \bar{u}^2 (1-\bar{u})\,dy < \varepsilon\delta_2 = \varepsilon\int_0^\infty \bar{u}(1-\bar{u})\,dy. \tag{26}$$
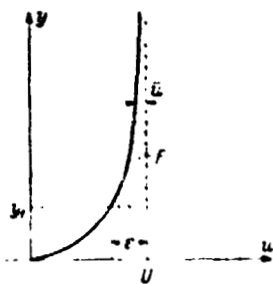

Fig. 3 Sketch for the Estimates Carried Out.

As long as $\vec{u} = 0$, i.e., as long
as no excess velocity is
present, this would be valid
if $\bar{u} < \varepsilon$ everywhere. This
surely is not true close to
the wall though. If we as-
sume, according to Fig. 3,
that in a range close to the
wall where $0 \leq y \leq y_1$ a share of
δ_{21} is already present of
pulse loss thickness while $\bar{u} \leq \varepsilon$ in the rest of the range then

14

$$\delta_2 \lesseqgtr \delta_{21} + F \tag{27}$$

when F, the share of displacement thickness δ_1, is outside of y_1. The left side of (26) can be estimated at the lower limit as

$$\int_0^\infty \bar{u}^2(1-\bar{u})\,dy > \int_0^{y_1}\bar{u}^2(1-\bar{u})\,dy = \int_0^{y_1}(\bar{u}-\varepsilon)\bar{u}(1-\bar{u})\,dy + \varepsilon\int_0^{y_1}\bar{u}(1-\bar{u})\,dy = (K+\varepsilon)\delta_{21}. \tag{28}$$

where K is probably a constant different from 0 and smaller than 1. Using estimates (27) and (28), (26) becomes

$$\tag{29}$$

or

$$(K+\varepsilon)\delta_{21} < \varepsilon(\delta_{21} + F)$$

$$F > \frac{1}{\varepsilon}K\delta_{21}. \tag{30}$$

Whenever a finite δ_{21} and a finite $\bar{u}_1$ is present for any v, H_{32} can only go toward the value of 2 when $F \to \infty$, i.e., when the share of displacement thickness far away from the wall, where $\bar{u} < \varepsilon$, increases toward infinity. Simultaneously with $(2-H_{32})$, $(H_{12}-1)$ also decreases towards zero because

$$(H_{12}-1)-(2-H_{32}) = \frac{1}{\delta_2}\int_0^\infty \bar{u}^3\,dy \leq \frac{1}{\delta_2}\left[\int_0^{y_1}\bar{u}^3\,dy + \varepsilon^3 F\right] = \frac{K}{\delta_2} + \varepsilon^3\frac{F}{\delta_2}. \tag{31}$$

Here $1/\delta_2$ decreases to 0 at least with ε for $2-H_{32}=\varepsilon \to 0$, because of (30), while F/δ_2 is limited. The entire right side of (31) decreases toward 0 with ε. From this follows

$$\lim_{H_{32}\to 2} H_{12} = 1 \tag{32}$$

15

This relation is not considered in the interrelations used so far (compare (21)), but can be introduced after some small changes that are in the uncertainty range of the entire inter-relation. For bleed-off calculations

$$H_{12} = \frac{11\ H_{32}+15}{48\ H_{32}-59} \tag{33}$$
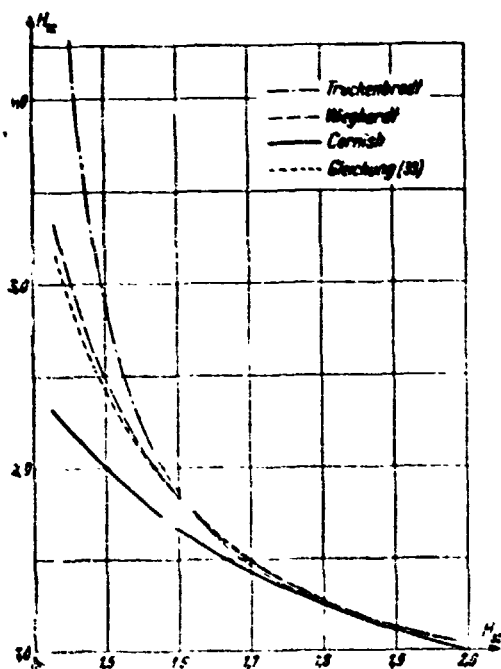
is recommended in place of statement (21).

Fig. 4 Various Interrelations of Form Parameters $H_{12}(H_{32})$ for a Turbulent Boundary Layer.

According to Fig. 4 there are hardly any differences between (21) and (33). They are effective only in the vicinity of $H_{32}=2$, in connection with the following derived basic laws for wall shearing stress. Other form parameter functions are also plotted in Fig. 4 for the sake of clarity. Significant differences are present only where H_{32} values are low. While the interrelation used by Truckenbrodt [7] provides slightly larger values of H_{12}, lower values are generated by another interrelation, based on data by Cornish, for the uncertainty region.

After extensive calculations with all three essentially different interrelations, which were partially reproduced by Seyb [17], the interrelation (33) was recognized as being useful in the normal range as well.

16

Theorem (19) for the wall shearing stress can also not be extrapolated in the present form for bleed-off examples. According to (1') wall shearing stress decreases toward zero for $H_{12} \to 1$ because of (30), since δ_2 increases toward infinite. This must be avoided. Apparently, very large contributions of F to δ_1 or δ_2 must be available for small values of $H_{12} \to 1$, derived from the regions far away from the wall with very small differences in potential flow. Those regions cannot have any influence on the wall shearing stress. A term must be added to (19), therefore, to take care that the values for $2-H_{32}=\epsilon$, which increase as $1/\epsilon$, not have any influence on δ_2. That is done through

$$\frac{\tau_0}{\varrho U^2} = 0.045716 \left((H_{12} - 1) \frac{U \delta_2}{\nu} \right)^{-0.232} e^{-1.260 H_{12}}.$$ (34)

The numerical constants in this relation are fixed so that there is the best possible agreement with the wall shearing stress theorems used so far, in the region of the most frequently occurring values of H_{12}. In Fig. 5 the comparison with (19) is shown for three values of $U\delta_2/\nu$ vs. H_{12}. The difference is appreciable only for values of H_{12} close to 1. For that region (19) was not derived. The boundary condition treated in (34) is represented here.

A further comparison of the wall shearing stress theorems is shown in Fig. 6. In addition to (19) lines according to Rotta [9] and Cornish [18] are plotted. The new theorem (34) is not essentially different from the others in the normal region. The straight lines are a little less inclined compared to (19), which is caused by the slightly lower exponent of the
Re number. That appeared expedient so as to improve the agreement with Rotta and Cornish for higher Re numbers.

Equation (2) for dissipation has been very reliable. It can already be seen for the laminar case that the form parameter has less influence on D^* than on ϵ^*. In the turbulent case it has so far been completely eliminated, according to (20).
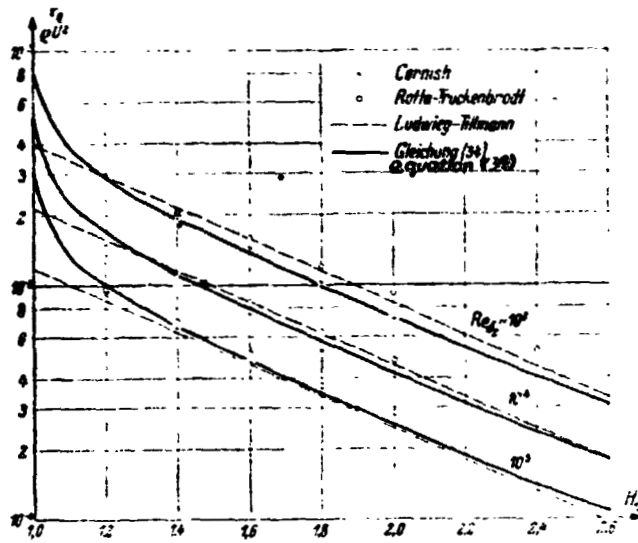
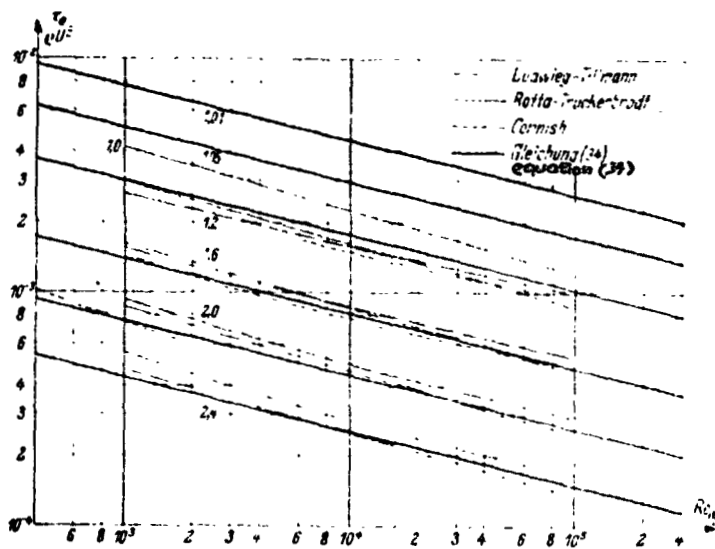Fig. 5   Turbulent Wall Shearing Stress as a Function of H_{12}.

Fig. 6   Turbulent Wall Shearing Stress as a Function of Re_{δ_2}

18

This can only be maintained approximately in the following treatment. since dissipation for $H_{32}\rightarrow2$ or $H_{12}\rightarrow1$ must also only be dependent on $(U\delta_2/\nu)^2(H_{12}-1)$, which is checked by means of (7). Instead of (20)

$$2\frac{d+\iota}{\varrho U^2} = 0.0100\left((H_{12}-1)\frac{U\delta_2}{\nu}\right)^{-\frac{1}{6}} \tag{35}$$

will be used subsequently, where the boundary condition is fulfilled and only an insignificant influence of H_{12} is present in the normal region. A large number of comparative calculation has furthermore established that dissipation has less influence on the results than shearing stress and that the boundary condition is more important than a really exact value. For all normal values of H_{12} (35) is,therefore,equivalent to (20).

5.   The Numerical Treatment

The differential equations (1) and (2) are completely defined for the laminar and turbulent case, with the relations derived in sections 3 and 4, and need only be integrated numerically. This can be done with known methods. Wherever the integration process will be discussed subsequently,it will be only to point out various characteristics of the differential equations themselves, which are used advantageously for the numerical treatment. Solved according to the derivations of the desired functions, equations (1) and (2) are as follows

$$\frac{d\delta_2}{dx} = -(2+H_{12})\frac{\delta_2}{U}\frac{dU}{dx} + \frac{\tau_0}{\varrho U^2} + \frac{\tau_0}{U} \tag{36}$$

$$\frac{d\delta_3}{dx} = -\frac{3\delta_3}{U}\frac{dU}{dx} + 2\frac{d+\iota}{\varrho U^3} + \frac{\tau_0}{U} \tag{37}$$

19

$$\frac{\tau_0}{\varrho U^2} = \frac{\varepsilon^*(H_{32})}{Re_{\delta_2}} \qquad \text{(laminar)}, \qquad (38)$$

$$\frac{\tau_0}{\varrho U^2} = 0.045\,716\,((H_{12}-1)\,Re_{\delta_2})^{-0.232}\,e^{-1.260\,H_{12}} \qquad \text{(turbulent)}, \qquad (39)$$

$$2\frac{d+\iota}{\varrho U^2} = \frac{2\,D^*(H_{32})}{Re_{\delta_2}} \qquad \text{(laminar)}, \qquad (40)$$

$$2\frac{d+\iota}{\varrho U^2} = 0.0100\,((H_{12}-1)\,Re_{\delta_2})^{-\frac{1}{6}} \qquad \text{(turbulent)}. \qquad (41)$$

As abbreviation the Reynolds number formed with δ_2 and U

$$Re \quad = \frac{U_{\delta_2}}{\nu} \qquad (42)$$

was introduced. The function $H_{12}(H_{32})$, needed in (37) and (38),
is defined by (16), resp. (21), ε^* and D^* by (17) and (18),
resp. Table I.

Equations (36) and (37) are apparently dimensionless since
velocities or lengths appear only simultaneously in numerator
and denominator. It is all the same, therefore, in which units
velocities and lengths are being measured. We introduce as
unit for the lengths l=1 and for the velocities U_∞=1, both
chosen to be most suitable for the particular task. All lengths
and velocities can consequently be considered as ratios of the
chosen units, resp. as functions made dimensionless along with
the units. This changes nothing in the entire formula system.
Only in the introduction, for convenience's sake, of the Re
number formed with the units

$$Re \quad = \frac{1 \cdot 1}{\nu}\,(=\frac{U_\infty 1}{\nu}) \qquad (43)$$

will in place of (42)

$$Re_{\delta_2} \quad = Re\ U\ \delta_2\,(=\frac{U_\infty 1}{\nu}\ \frac{U\delta_2}{U_\infty 1}) \qquad (44)$$

be used in the future.

20

The α.fferontial equations (36) and (37) have the form of

$$\frac{d\delta_2}{dx} = f(x,\delta_2,\delta_3), \quad \frac{d\delta_3}{dx} = g(x,\delta_2\delta_3),$$

where the only difference between laminar functions f and g in the laminar and turbulent cases is that for wall shearing stresses, energy dissipation and form parameter, sometimes equations (38), (40) and (15), and sometimes (39), (41) and (21), must be used. $U(x)$ and $v_0(x)$ are given functions, dU/dx can easily be formed during integration.

For step-by-step integration Runge's second order method is most suitable. With initial values x_1, δ_{21}, δ_{32}, U_1, v_{01}, final values $X_2 = x_1 + \Delta x$, and analog $U_2^{\cdot}, v_{02}$ given, the differences between the desired variables are calculated by means of

$$\Delta\delta_2^{(1)} = f(x_1, \delta_{21}, \delta_{31}) \Delta x, \quad \Delta\delta_3^{(1)} = g(x_1, \delta_{21}, \delta_{31}) \cdot \Delta x$$
$$\Delta\delta_2 = f\left(x_1 + \frac{1}{2} \Delta x, \ \delta_{21} + \frac{1}{2}\Delta\delta_2^{(1)}, \delta_{31} + \frac{1}{2} \Delta\delta_3^{(1)}\right) \Delta x, \quad \Delta\delta_3 = g(...) \Delta x$$

For hand calculation little schedules for the calculation of the right-hand sides f and g must be made. Often it will be noticed that after the first half-step a repetition of the calculation will have no significant influence and so this step can be eliminated.

On occasion one will observe another, much more unpleasant, characteristic of the solution. Differences fluctuate in a strange way rather heavily around the true value, particularly when the boundary layers are still thin, as for stagnation point flows or in the vicinity of an intake. The reason for it is that neighboring solutions, to which one turns because of inaccuracies or mistakes in rounding off, tend strongly toward

the desired solution, particularly for H_{32}. The step-by-step
integration follows, according to Fig. 7, by going halfway in
the direction toward the tangent to the point of departure
then calculating the tangent direction and following in the
tangent direction for completion of the entire step. When the
neighboring solutions tend too strongly toward the solution, as
sketched in Fig. 7, the error during one step increases greatly.
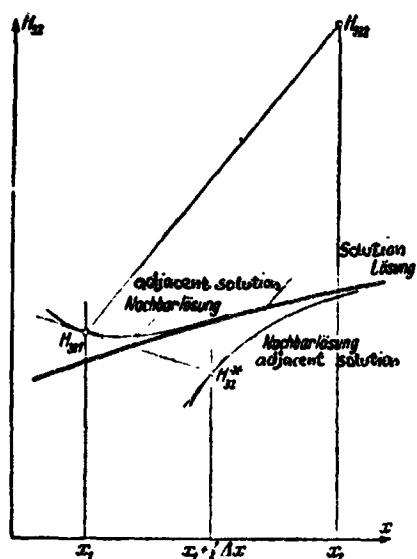

Fig. 7 Sketch of the Numerical
Instability Occurring.

The reason for numerical instability is not based on this particular approach to a solution but is characteristic for differential equations (36) and (37) and, therefore, in more or less apparent fashion built into all previous studies based on the pulse and energy theorem. The better the applied numerical method, the more the instability becomes apparent. For that reason alone it was not discovered in the previous studies.

It is apparently of little use to employ a method of a
higher order, like that of the fourth degree by Runge-Kutta, to
remove the instability. In that case the instability can even

22

greatly increase. The successive step decrease has so far been
the most reliable, generally applicable, way. As long as the
numerical calculation is carried out by hand and one can survey
not only the fluctuations but the entire calculation constantly
other paths are open. From time to time a check can be made
whether the initial calculation, for stagnation point or intake,
for instance, as discussed later, can be further extended.
Often that can already lead away from the instability region
but it must not be considered as panacea. An uncritical ex-
tension of the initial step can lead to serious errors. When
programming instructions for calculations on digital computers,
which are very suitable for it, checks must be built into
every step, for recognition of numerical instability. When
it occurs only a decrease of the step length is still indi-
cated, best to half. The required criteria will now be pro-
vided, briefly. All other details of programming need no
further explanation. We designate a few of the functions that
occur in the course of the integration step

$$H_{321} = \frac{\delta_{31}}{\delta_{21}}, \quad H^*_{32} = \frac{\delta_{31} + \frac{1}{2}\Delta\delta_3^{(1)}}{\delta_{21} + \frac{1}{2}\Delta\delta_2^{(1)}}, \quad H_{322} = \frac{\delta_{32}}{\delta_{22}}.$$

After that there should be stabilization with

a) $|H_{321} - 2H^*_{32} + H_{322}| > \epsilon_1 \quad (\epsilon_1 \approx 0{,}0001 \text{ bis } 0{,}01)$,

b) $H^*_{32} > 2$,

c) $H_{322} > 2$,

d) $\delta_{21} + \frac{1}{2}\Delta\delta_2^{(1)} \leq 0$,

e) $\delta_{22} < 0$.

The excluded possibilities from (b) to (e) occur normally any-
way only in cases that already fulfill the condition (a) and
thus aim for a step decrease. They must be recognized before
check (a) only because they might require [as in (39)] useless
calculations which would lead to a stop of the computer before
check (a). Once the step decrease has been programmed ; ̇ ̇
no trouble to catch all these absurd cases and to chang   ᵧ
to step decrease if need be.

Quite a few other refinements ᵧf the calculation can be
achieved through step decrease. For instance, H_{32} often de-
creases steeply in the vicinity of separation points, creating
some inaccuracies with it. This makes it advisable to limit
the entire contribution to change of H_{32} and to carry out the
step bisection when

f) is $|H_{322}-H_{321}| > \varepsilon_2$ ($\varepsilon_2 = 0.01$ to 0.03).

Naturally, the bisectioned steps are checked again for
fluctuations of differences that are too strong and bisectioned
again, if needed. This bisectioning process should be carried
on at random, a lower limit being set for $\overline{\Delta}x = (1/2)^n \Delta x$ which,
in order of magnitude, is 1/1000 of the smallest initially oc-
curring step size. Going below this limit may stop the program.
It has been shown that a large number of programming errors can
be laid to continued step bisectioning. These errors are found

24

easiest after the program is stopped because the step c... s
have become too small. If one were to try to continue the cal-
culation the search for errors would at best be made more dif-
ficult, since memory locations are overwritten where errors
could otherwise be recognized.

During bisectioning of the examples shown later U and v_0
were linearily interpolated, i.e., held constant over the en-
tire initial step dU/dx, even though it was subdivided into
perhaps 32 or 64 partial steps $\overline{\Delta}x$. This is justifiable when
the step size of the particular problem was chosen so small
that linear interpolation between supporting points is mean-
ingful within the context of this problem. With the integra-
tion method chosen it leads to a second order approximation
when the output interval Δx is handled without bisectioning.
A step decrease is, after all, introduced for elimination of
purely numerical instability and not for increase of calcula-
tion accuracy. It is easiest to increase the number of support
points if there is concern about the linear interpolation.
Better interpolation of U and dU/dx is not a principal diffi-
culty, however. It is to be used with care only when dU/dx
shows nonuniformities, which happens often in practice.

The numerical integration of differential equations has
now been taken care of. Calculation by hand is very simple;

25

just the same it is more effective to program it so as to obtain far more voluminous result material at considerably lower cost. A few matters have to be considered, as always during programming, which do not become conspicuous during calculation by hand since there is constant monitoring of the calculation flow and immediate intercession when something is not quite normal. Now there remain only a few special cases, at the start of the calculation, at the boundary layer shift and at the separation, to be discussed.

6.   Initial Values

The integration of the differential equation system (36), (37), so far discussed, does not assume disappearing values for U, δ_2 and δ_3. These conditions are not fulfilled at the start of a boundary layer. The two most important cases are the "shockfree approach" of the potential flow at a sharp edge and the stagnation point flow. In both cases considerations of the boundary are required, the first steps of the boundary layer calculation being easily carried out with their results.

a.   Shockfree Approach

In this case the boundary flow starts with a U that does not disappear. It is shown through well known procedures that the boundary layer then starts with disappearing δ_2 and δ_3. In (36) and (37) only those terms with the smallest powers of δ_2 and δ_3 are of importance for small values of δ_2. If the others are neglected then

$$\delta_2 = \left| \frac{\nu \cdot x}{Re} \right| \cdot$$
(45)

$$\cdot \cdot 2 \, D^* \cdot$$
(46)

26

Equation (46) provides a value for H_{32}, which is exactly the one that also holds true for the plate flow U=constant. Since we have obtained the interrelations of the form parameters (16) and (18) from the similar boundary layers, which contain the plate flow, (46) must be fulfilled for the H_{32} value of the plate flow, namely H_{32}=1.57258. That can be checked easily with Table I and the equations (16) and (18). It also serves for easy calculation of δ_2 from (45). By putting the value of ϵ^* that belongs to H_{32}=1.57258 into the equation at the onset of flow where x=0 and U=U_o,

$$\delta_2 = 0.66411 \sqrt{\frac{x}{Re\ U_o}} \quad . \tag{47}$$

δ_3 is also known through (11) and the equations (36) and (37) can be further integrated numerically.

b. Stagnation Point

In the vicinity of the stagnation point U=U'x. It is shown that the functions δ_2 and δ_3 must be constant for small values of x and for v_o=0. The well known boundary consideration then furnishes

$$3 H_{32} \epsilon^* \quad 2 (2 + H_{12}) D^* \tag{48}$$

and

$$\delta_2 \quad \left| \frac{3 D^*}{2 H_{12} Re\ l} \right. \tag{49}$$

Although the boundary consideration proceeds independent of v_o during the inflow, $v_o \neq 0$ would change equations (48) and (49). But since bleed-off is hardly used in the vicinity of the

---

*From 48. See [17].

27

stagnation point it is sufficient to neglect it for at least a small part of the way in initial calculations.

If the same form parameter interrelations had been used for $H_{32}>1.57258$ as for the similar boundary layers free of bleed-off then (48) should be fulfilled for the exact value of H_{32} at the stagnation point flow, namely $H_{32}=1.62575$, which would give $\delta_2=0.29234/\sqrt{Re\ U^r}$. But since more consideration must be paid to bleed-off in this region, condition (48) is fulfilled for (16), (17) and (18) when $H_{32}=1.61998$, which leads to

$$\delta_2 = 0.29004 \frac{i}{\sqrt{Re\ U^r}} \tag{50}$$

The deviation in δ_2 is unimportant, being less than 1%, but is more significant in H_{32} since there is no way to compare the absolute amounts. When referred to the H_{32}-region between separation (1.51509) and asymptotic bleed-off at the plate (1.66667) the deviation in H_{32} amounts to 3.8%, which is tolerable in relation to other methods of approximation.

This error is, incidentally, a basic one for all methods with one parameter. It stems from the fact that in reality different boundary layer profiles can belong to the same form parameter H_{32} and so can different values for ϵ^* and D^*, while in this case a special relation was selected. According to a suggestion by Seyb [1] one might attempt to use various functions H_{12}, ϵ^* and D^* for cases with or without bleed-off. That would certainly allow significantly improved accuracy in the handling of many other examples, for instance the stagnation point flow and also the flat plate with blow-off, which is particularly poorly covered in section 8. It is questionable, however, if that will always involve higher accuracy, particularly for examples where there is only partial bleed-off.

28

The error at the stagnation point flow may be taken as indication óf the general shortcoming of the method, even though it is problematical to judge the efficiency of a method from special examples. Examples with much smaller errors will be calculated but some with considerably larger deviations can also be constructed. Such a one is the flat plate with blow-off. In practice it is unimportant but it clearly demonstrates the limits of the method.

7. Boundary Layer Separation, Boundary Layer Shift

a. Laminar Separation

The separation point of the laminar boundary layer is defined by disappearing wall shearing stress. The disappearing wall shearing stress is assigned to the value $H_{32}=1.51509$, since a clear relation between the functions ε^* and H_{32} was introduced in the present method.

It is no problem for calculation by hand to fix the exact point where H_{32} reaches the separation value, either by extrapolation or by change of step sizes.

For computer programming there are again certain considerations, since $H_{32}<1.51509$ can never be entered into equations (16) to (18) because that would lead to a root with negative radicand and again to a computer stop. The following method has been shown to be the must reliable one. A check is made after each half-step whether $H_{32}^*<1.51509$ or $H_{322}<1.51509$. If yes, new values for $\overline{\Delta}x$ must be obtained by the Regula falsi (approximation method for obtaining the solution of an equation) with the aim to repeat the step with the changed $\overline{\Delta}x$ so that in the end $H_{322}=1.51509+\varepsilon$. If the separation boundary is again transgressed after this step the Regula falsi is used again for

29

calculation of a somewhat smaller step size, if $H_{322} \gtrsim 1.51509$
calculation is continued. It only remains to check before each
partial step that $H_{32} < 1.51509 + 2\epsilon$. If so then the starting
point of the partial step is the laminar separation point.
Function ϵ is only a threshold value, which prevents the pro-
gram from getting lost in a rounding off error. At the same
time the accuracy with which the separation point is determined
can be gauged with ϵ. With $\epsilon = 0.5 \cdot 10^{-5}$ that accuracy should be
good enough. With this value very few step decreases are re-
quired until the point of separation is found.

If the calculation is not finished after the laminar sepa-
ration, but continued for the turbulent case, it must be
remembered that the $\overline{\Delta}x$ of the preceding calculation step did
not result any longer from step bisectioning. In contrast to
step reduction through stabilization one would not come to the
final point of the total step if one were to continue the calcu-
lation with the existing $\overline{\Delta}x$. For that reason the entire piece
between the separation point and the end of the integration
step is used as $\overline{\Delta}x$ after the laminar separation. After that,
step bisectioning through stabilization is again permissible.

b.   Turbulent Separation

Turbulent separation still presents a big uncertainty
today. It is generally assumed that separation can occur for
$H_{32} = 1.58$ and that it definitely has happened for $H_{32} = 1.46$.
These boundaries can be considerably extended (upward and down-
ward) particularly for bleed-off. Fortunately, the uncertain-
ties are not quite as big as it may appear at first glance from
the H_{32} values. According to Seyb [19], and to one of my inves-
tigations [20], the turbulent boundary layer does not permit a
layer gradient any longer, if the value of H_{32} is permitted to

30

drop below 1.58 (without bleed-off). The result is, conversely, that for $H_{32} < 1.58$ the influence of the pressure gradient of the form parameter is very sensitive. In many cases the change of H_{32} in that region is so great that only a small distance lies between the two points at which the values of $H_{32} = 1.58$ and $H_{32} = 1.46$ are reached, there being little influence on the point of separation by the chosen value of the separation parameter. For bleed-off, however, the influence of the amount bled off is quite critical, so that one can stay on the safe side without much additional bleed-off.

All the examples shown here were calculated up to the value of $H_{32} = 1.46$. A decision must be made in each case whether another separation criterion would have had significant influence.

The location of the point where $H_{32} = 1.46$ is reduced can be exactly as in the laminar case, but the check after the first half-step can be eliminated since no stop of the computer occurred even for $H_{32} < 1.46$.

Reasons for continuation of the calculation may remain even after the turbulent separation, but the size of the remaining step must then be readjusted. Often the friction drag, after Squire and Young [21], is calculated after a boundary layer calculation. This formula is valid only up to the separation point, of course. For technical reasons of programming it is simpler, however, not to calculate the drag part immediately at the separation point but through

$$\delta_{22} = \left(\frac{U_s}{U_\delta}\right)^{\frac{5+H_{32}}{2}} \delta_{21}$$

to provide for continuation of the calculation after the separation, in a way that leaves the drag after Squire-Young

unchanged. At the end of the entire calculation it can be
obtained uniformly,

c. Boundary Layer Shift

The boundary layer shift is considered in the present
method simply by using equations (33) and (35),instead of
(16) and (18) for calculations from a certain point on. A
sudden increase in H_{32} at the shift point, as was required in
other methods to some extent [7], is eliminated. Later on
the examples will show that in most cases, but not always, a
strong increase in H_{32} occurs after the shift. It seems sig-
nificant that this increase is the result of the relations
used only and must not be introduced artificially. Those cases
where no rapid increase of H_{32} occurs appear also of importance
in practice, which is pointed out during discussion of the ex-
amples.

Where the shift takes place is of no special relevance to
the method discussed. It should be pointed out, however, that
the most varied shift conditions can be introduced in a simple
manner. The laminar separation point will be introduced as
the latest shift point. It has been shown to be a good prac-
tice to continue the calculation from the laminar separation
point on principle as for the turbulent case. Additional
simple shift conditions that are often used are shift when

$$U_2 - U_1 < 0 \qquad\qquad\qquad \text{(UB1)}$$

or

$$U_2 - U_1 \lesssim 0 \qquad\qquad\qquad \text{(UB2)}$$

32

That means shift at minimum pressure. A difference between
(UB1) and (UB2) exists only when U is constant over a finite
distance. The transition from (UB1) to (UB2) permits calcula-
tion of the influence, in this case of the advancing migration
of the shift point from the end to the beginning of the distance
with constant velocity. This influence is important for laminar
profiles. It determines the depth of the so-called laminar de-
pressions in the polar diagram.

It will be important for many calculations to consider
the instability of the laminar boundary layer. It depends
mainly on the form parameter and on the Re number. The results
of various stability calculations are plotted in Fig. 8. There <u>/236</u>
is some dispersion, depending on the exact shape of the boun-
dary layer profiles on which they are based. The boundary of
stability is higher, for instance, according to the mean by
Ulrich [22], for the Iglisch-profiles of homogeneous bleed-off
than, according to Pretsch [23], for the Hartree-profiles. A
certain amount of dispersion is contained in the methods of
calculation as well because two different values are given for
the stability boundary of the so-called Blasius-profile, which
is mentioned in both categories as a special case. Wieghardt
[6] carried out a rough interpolation for his calculated values,
therefore, which has been included in Fig. 8.

The stability boundary alone does not suffice for predeter-
mination of the shifting point, however, since a certain dis-
tance is always required between the onset of instability and
the shift. The unstable waves must reinforce themselves con-
siderably at first until their amplitude is sufficient for the
shift over into the completely irregular turbulent motion.
During this unstable interval of operation δ_2 usually increases
to such an extent that the motion moves, in Fig. 8, from the
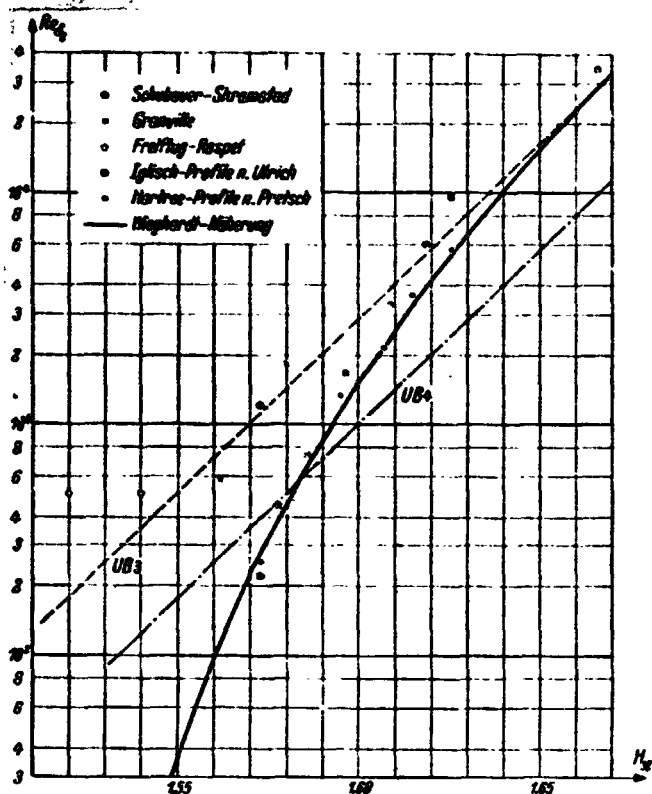stability boundary away upward, becoming more unstable. For

Fig. 8 Theoretical Instability Boundaries, Experimentally Determined Data for Boundary Layer-Shift and Introduced Shift Conditions.

a constant form parameter, the Blasius flow for instance, only δ_2 will increase but in many cases of pressure increase a decrease of H_{32} will accompany the increase in δ_2. The shift will take place, therefore, somewhere above the stability boundary in Fig. 8 with the degree of turbulence of the outside flow and the wall roughness playing a certain role, of course.

Experiments provide a certain indication about the practical occurrence of the shift for the least disturbance of the flow and the wall. Some experimental results have been entered in Fig. 8 for that reason. Schubauer and Skramstad [24] made their careful experiments with the flat plate, i.e., without a change in the form parameter. Granville [25] investigated the shift for laminar profiles and found a rather clear relation for the difference in Re numbers for instability and shift and the mean form parameter during the unstable interval of operation.

$$\Delta Re_{\delta_2} = Re_{\delta_2}(\text{shift}) - Re_{\delta_2}(\text{inst.})$$

By exchanging the mean form parameter with that at the shift point, which is, strictly speaking, only correct for a constant

34

form parameter, data points from Granville can be plotted in
Fig. 8. This was done only for two characteristic values. More
recent experiments by Raspet [26], for free flight for instance,
show that the shift occurs even later for smaller Re numbers.
Two data points from Raspet's experiment are plotted in Fig. 8.
On the other hand, it must be expected that the region of high
Re numbers and, with it, high form parameter values can only be
reached through bleed-off. The relation between H_{32} and δ_2 may
change completely in that case. For example, bleed-off may
proceed in such a way that the motion takes place always along
the instability boundary (see examples in section 8) or paral-
lel to it so that there is no move away from the boundary of
stability during the unstable interval of operation in Fig. 8.
It must at least be taken into account that the shift takes
place close to the boundary there. For that reason the straight
line plotted in Fig. 8

$$\ln Re\delta_2 > 34.2 \; H_{32} - 46.78 \qquad \text{(UB3)}$$

is recommended as shift condition if one wants to hit the shift
approximately as it occurs in practice. But if a certain pre-
vention of the shift is required then the also plotted straight
line

$$\ln Re\delta_2 > 34.2 \; H_{32} - 47.81 \qquad \text{(UB4)}$$

is used. If no shift appears in a calculation with this condi-
tion then one can be reasonably sure that the experiment will
also remain laminar.

The choice remains, of course, to introduce different
shift conditions. Each condition introduced will normally be
checked before the calculation of an integration step. An

exact check is not necessary for hand calculations until it becomes apparent that the boundary is being approached.

8. A Few Bleed-Off Theorems

The principal boundary layer data can be calculated with the methods described, when the normal velocity $v_0(x)$ is given in addition to the always provided functions Re and $U(x)$. Often it is also the other way around, namely $v_0(x)$ is to be calculated so that the boundary layer will fulfill certain conditions; for instance, the prevention of shift of the boundary layer or of the separation of the turbulent boundary layer.

This problem is also solved easily with the equations described and with the associated methods of calculation and programs. Several different aims of bleed-off are jointly attained when the requirement is to fix the bleed-off velocity v_0 so that

$$H_{32} = \psi(\delta_2) = a + b \ln \mathrm{Re}\delta_2 \tag{51}$$

Constant H_{32} for the laminar and for the turbulent case is designated by b=0. But if one chooses a=1.40, b=0.2924, then one is always right below the condition for certain shift in the laminary case of Fig. 8 and so prevents the boundary layer shift. In the turbulent case there are also a few possibilities with b≠0, which are explained through examples.

Using (11) in (51) we get

$$\delta_3 = (a + b \ln Re_{\delta_2}) \delta_2 = \psi(\delta_2) \delta_2 \tag{52}$$

and through derivation

$$\frac{d\delta_2}{dx} = [a + b\,(1 + \ln Re_{\delta_2})]\,\frac{d\delta_2}{dx} + b\,\delta_2\frac{1}{U}\frac{dU}{dx}. \tag{53}$$

With these two relations the functions δ_3, $d\delta_3/dx$ and $d\delta_2/dx$
can be eliminated from (36) and (37) and one gets

$$(b + \psi - 1)\frac{v_0}{U} = 2\frac{d + l}{\varrho\,U^3} - (b + \psi)\frac{\tau_0}{\varrho\,U^2} + [b - \psi + H_{12}\,(b + \psi)]\frac{\delta_2}{U}\frac{dU}{dx}. \tag{54}$$

This makes v_0 a function of dU/dx and δ_2; with δ_2 one also gets
H_{32} because of (51) and the required boundary layer functions
can be calculated as before. For continued calculation only
the change of δ_2, given with (36), is required and the differ-
ential equation (37) is not needed. This exactly corresponds
to the accepted procedure as given by Wieghardt [6], for
instance.

This procedure does require, however, that the equation
be already fulfilled at the spot where the calculation with
the bleed off theorem (51) is to start. But normally, values
for the pair of functions δ_2, H_{32}, are already present from a
previous calculation at that starting point, which may not be
compatible with (51). That difficulty can be eliminated by
treating (54) and (51) together only as additional equation
to $v_0(\delta_2)$ and by carrying out the actual boundary layer calcu-
lation again with the two equations (36) and (37), with no need
for agreement between the H_{32} used and ψ. Because this pro-
cedure uses the bleed-off theorem only for v_0 and not for H_{32},
it is questionable whether and how fast H_{32}, which is generated
in the course of the calculation, adapts itself to the value of
ψ per (51). As the examples will show, that happens very well
and rather quickly.

This procedure does require a bit more calculation effort
than that by Wieghardt, since boundary layer functions for the

values ψ and H_{32} must be calculated. As long as the two values
are not equal this double calculation cannot be av..:ded. When
calculating by hand equation (37) can be dropped as soon as
there is close enough proximity between ψ and H_{32}. For pro-
gramming this transition is not necessary. This keeps the
program in its old form, which is beneficial for functional
clarity. Possible time savings in calculation do not justify
the effort involved. Besides, the condition $v_0 \leq 0$ is possible
for the recommended method, which is appropriate to many prob-
lems. According to it bleed-off takes place only when the bleed-
off theorem really requires it and not when, for instance,
the boundary layer is brought to the edge of the stability
boundary artificially, through blow-off, when normally it
would still be far away perhaps near the stagnation point.

9.   Examples

It should again be pointed out that the unit of length in
all following examples is that which is also used in the
Reynolds number Re, according to equation (43). The same
holds true for the unit of velocity. If one wanted to reintro-
duce the designations 1 and U_∞ later for the units, then all
functions would have to be represented as ratios to these units.
But that is superfluous. The only thing to be kept in mind is
that for x=1 the unit of length, 1, is meant, from (43), which
can also be designated as 1; the same is true for all veloci-
ties.

a.   Parabola-shaped Velocity Distribution for Different
Step Sizes

To provide an example for the influence of linear interpo-
lation on U within one integration step, the curved distribu-
tion $U(x) = x(2-x)$ for $Re = 10^6$ with widely varying step sizes was
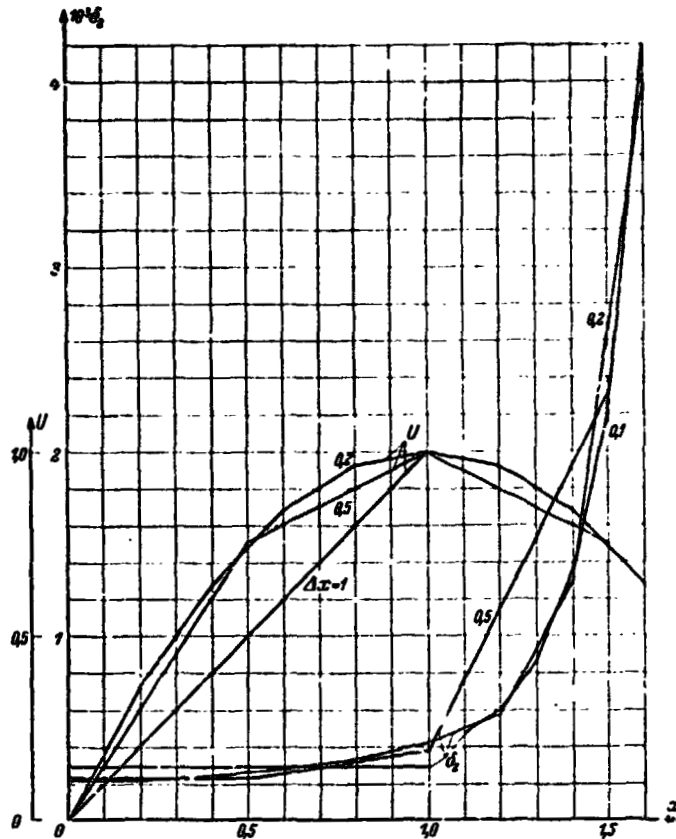
38

Fig. 9   Influence of Step Size on Pulse Loss Thickness δ_2

calculated.   Consecutively, $\Delta x = 1, 0.5, 0.2, 0.1, 0.02$ and 0.01 was

chosen.   Results for the four biggest step sizes are shown in

Fig. 9.   The comparison was demonstrated only on δ_2.   The errors

in H_{32} are smaller.   The data points for U used and those calcu-

lated for δ_2 were always joined by straight lines to character-   /239

ize the step size.   The effect of decreasing Δx to below the

value of 0.1 can no longer be shown graphically.   For that

reason the results were put together in Table II for the two

points $x = 1$ and $x = 1.6$ with their errors.

The step size 0.1 already shows good results when a total
of only sixteen steps is counted in the interval. But gross
errors must be expected when the velocity increase is linearized
too roughly and the stagnation point solution too far extended,
which often happens.

Table II

**Pulse Loss Thickness for U=x(2-x), Re=10⁶ for x=1 and
x=1.6 as Functions of Step Size**

.x	10⁴ δ,(1.0)	(δ/δ₀)·	10⁴ δ,(1.6)	(δ/δ₀)·
1	2,400	31.7		
0.5	3.766	11.3		
0.2	4.139	2.5	40.24	6.7
0.1	4.214	0.7	41.81	3.1
0.05	4.223	0.5	42.67	1.1
0.02	4.243	0.05	43.06	0.1
0.01	4.245		43.13	

b. Howarth-Flow with Turbulent Continuation

The velocity distribution U(x)=1 was treated rigorously by
Howarth [27] and recalculated accurately by Leigh [28]. This
calculation often served for comparisons with the results from
approximation methods (Walz [5], for instance). In particular
the point of laminar separation is very critical and could
heretofore not be calculated with satisfactory accuracy by ap-
proximation methods. The equations and functions now available
produce an error that is smaller by an order of magnitude. A
graphic comparison with the exact solution is no longer pos-
sible because the lines do not provide sufficient difference
for it. Numerical values for the separation point are shown
for various methods in Table III. It comes as surprise that
the present procedure offers much better results than that by
Walz even though the basic equations and the boundary line
profiles on which functions H_{32}, ϵ^* and D^* are based are the
same ones for the laminar case. As mentioned before, it was
found that the functions used by Walz had been incorrectly

40

Table III

Separation Point for Howarth-Flow in Various Directions

Procedure	x (Separation)	Error %
Howarth-Leigh	0.1198	0.0
Pohlhausen P4	0.16	33.0
Pohlhausen with Hartree profiles	0.103	14.2
Walz with Pohlhausen P4	0.125	4.2
Walz with Hartree profiles	0.114	5.0
Wieghardt 2 parameter method	0.116	3.3
Görtler (difference method)	0.1183	1.2
Prel. method with Walz-Hartree function	0.1137	5.0
Prel. method with new Hartree functions		
$\Delta x = 0.01$	0.1202	0.4
$\Delta x = 0.002$	0.1199	0.1

calculated. With the interrelations for H_{32}, ϵ^* and D^* used by Walz the same results are achieved here as there, with the present formulas. Further improvement can only be attributed to accurate evaluation of the Hartree profiles. The actual statement by Walz is significantly better, therefore, as can be concluded from the results up to now.

Fig. 10 also gives the curve of the form parameter H_{32} for various Re numbers. The laminar separation point was here assumed as shift point. In the laminar part H_{32} is independent of Re, which can already be deduced from the basic equations, but that is not true in the turbulent part. In Fig. 10 it can be clearly recognized how H_{32} increases rapidly with the higher Re numbers after the shift, at approximately the rate at which Truckenbrodt [7] introduced it artifically. But for smaller Re numbers the jump does not occur. Here H_{32} still moves for awhile after the shift in the region $H_{32} < 1.58$, where separation

is already possible. This result agrees with the observation
that local separation is often found [29] before the boundary
shift, for smaller Re numbers. According to Fig. 10, the
reason for this separation bubble must not only be sought in
the insufficiency of excitement of the unstable disturbances,
but also in the too slow formation of the turbulent boundary
layer and with it the removal of flow reversal danger at the
wall for this range of Re number and form parameter.

Additional calculations with uninfluenced turbulent boun-
dary layers have already been carried out in large numbers,
also comparisons with experiments. Two of these comparisons
have been published previously [14]. There it is shown, in
particular that the increase of δ_2, according to the much
applied method by Truckenbrodt for the area of high pressure
increase, seems too small while better values are achieved
with the equations presented here. One considerable improve-
ment of Truckenbrodt's method,mertioned by Scholz [10],does
correct the shortcoming for the pressure increase in the turbu-
lent region but generalization of this improvement for the
laminar case and for bleed-off has not been tried so far.

c. Laminar Plate Flow with Homogeneous Bleed-Off and Blow-Off

A further classical example, for which an exact solution
is available, is the flat plate $U=1$, with constant bleed-off
v_0. The recalculation of this case, which is shown in Fig.
11, also provides very accurate results. Iglisch's [30] solu-
tion agrees in δ_2 almost completely with the present one,
there being only insignificant differences for H_{32}. To achieve
such good agreement the step size of the first step Δx, which
is calculated without bleed-off here, must be kept very small
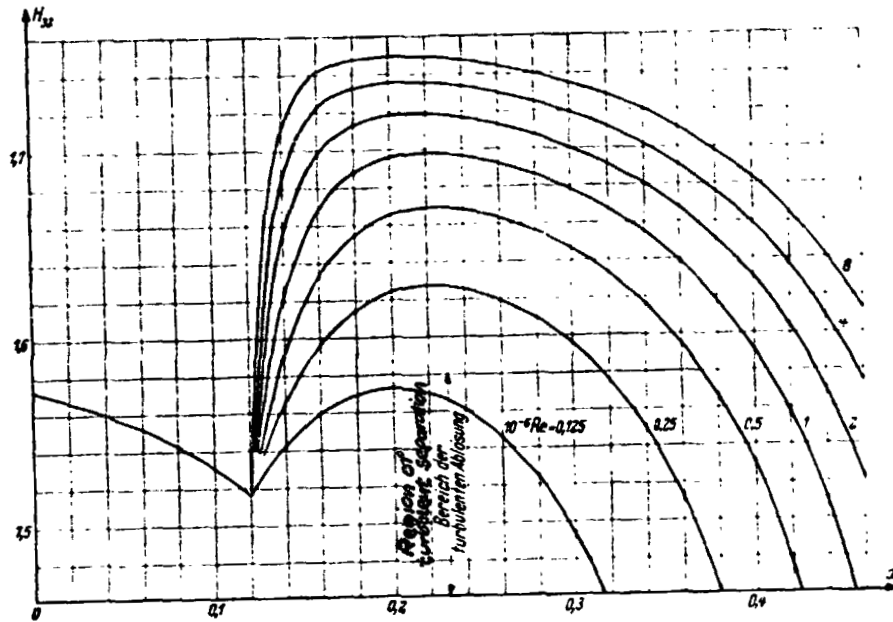
42

Fig. 10   Form Parameter H_{32} for Howard-flow U=1 and its Continuation for different Re numbers.
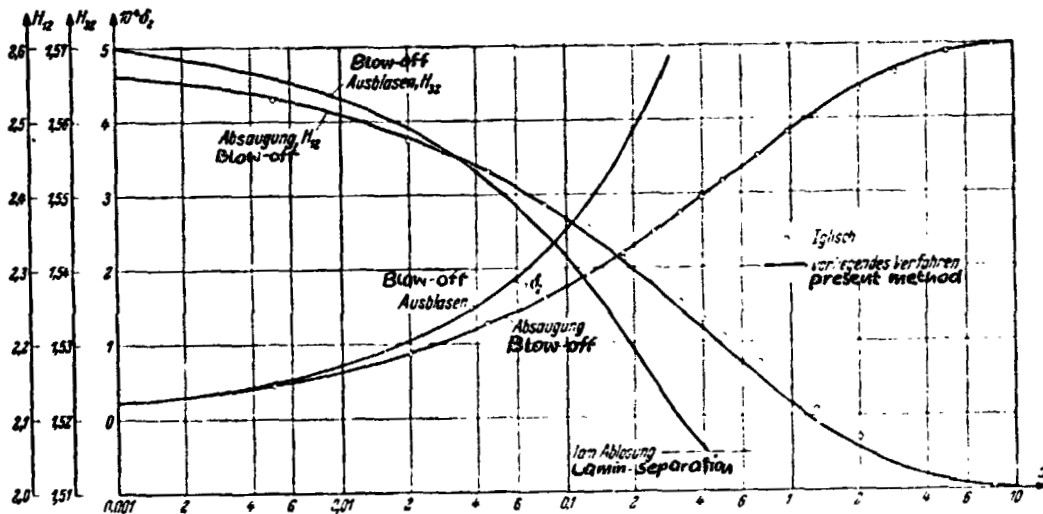

Fig. 11   Form Parameter H_{32} and Pulse Loss Thickness δ_2 for Plate Flow with Constant Bleed-Off and Blow-Off.   Re=10 , $v_0 = \pm 0.001$.

43

since the influence of bleed-off is particularly significant there.

For comparison, the lengths that were made dimensionless by Iglisch are recalculated. In the function used there

$$\xi = \left(\frac{v_0}{U_\infty}\right)^2 \frac{U_\infty l}{\nu} \frac{x}{l}$$

only the Re number need to be introduced, per (43), along with the units 1 and U_∞; the interrelation between the values chosen here for v_0 and Re, and ξ and x, can then easily be established. The same holds for function

$$-\frac{v_0 \delta_1}{\nu} = \frac{-v_0}{U_\infty} \frac{\delta_1}{l} \frac{U_\infty l}{\nu}.$$

The same case of plate flow but with positive v_0, i.e., blow off, is shown also in Fig. 11. As in all approximation methods, laminar separation occurs for x=0.4, which cannot occur for rigorous treatment. That is the case mentioned in section 5(b) in which the present method does not work too well. In practice it is unimportant since the blow-off profiles are anyway very unstable and boundary layer shift cannot be avoided here. Still, it may serve as an example of how little significance errors found in special cases have for the entire method. As far as the laminar part is concerned in the present method, it must be concluded from results up til now that it offers very good results when pressure increase without bleed-off or bleed-off to high values of H_{32} is involved. This exactly corresponds to the choice of functions H_{12}, ϵ^* and D^*, made in section 3. For more detailed investigations of errors we refer to Nickel [31].

44

d. Plate Bleed-Off with Constant Form Parameter

In Fig. 12 the distributions $\delta_2(x)$ and $v_0(x)$ for the flat
plate with constant form parameter, which have been obtained
with the present method, are compared with the exact solutions.
Again very good results are generated for $H_{32}>1.57258$. That is
only natural because the form parameter interrelation was taken /242
from the corresponding exact solutions. On the other hand for
blow-off, i.e., for H_{32} values below 1.57258, results would be
somewhat worse because for that region other in⁺errelations for
form parameters were chosen. Since blow-off is not allowed in
the programs used here, for reasons already mentioned in sec-
tion 8, blow-off cases of the "similar" plate flow (anyway
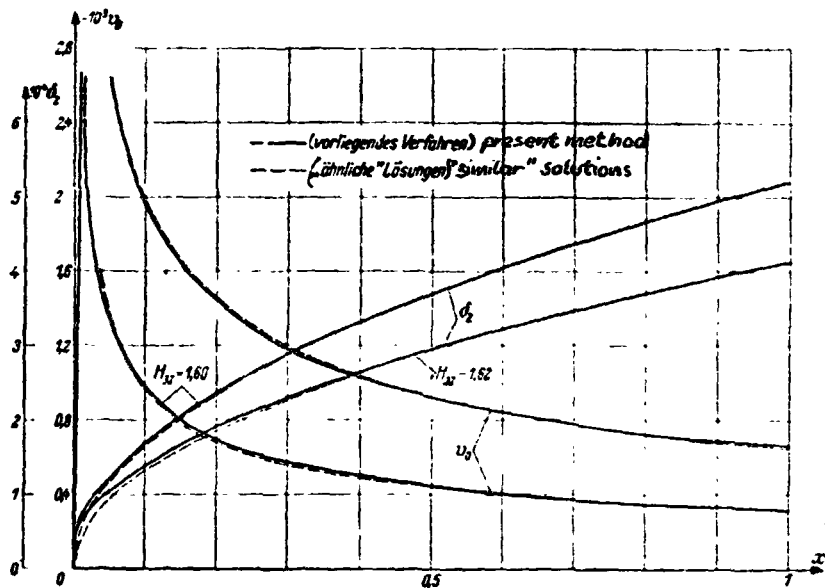again largely unstable) were not calculated.

Fig. 12 Recalculation of Bleed Off Velocity v_0 for Similar
Bleed-Off Boundary Layers at U=const., Re=10^6.

e. Bleed-Off of Laminar Boundary Layer for Strong Pressure Increase

An important area of application for bleed-off is the prevention of boundary separation, for instance on air foils with high lift coefficients. Large negative pressures and, subsequently, long and strong pressure increases occur on the topside. To get an overall picture for the bleed-off required in such cases a large number of calculations were carried out for a velocity distribution composed of linear sections, shown in Fig. 13. The pressure increase in the distribution on which it is based goes from U=4 to U=0.4, thus attaining a value that could never be overcome without bleed-off. This order of magnitude approximately corresponds to what occurs on air foils with very high lift coefficients (between 3 and 5).
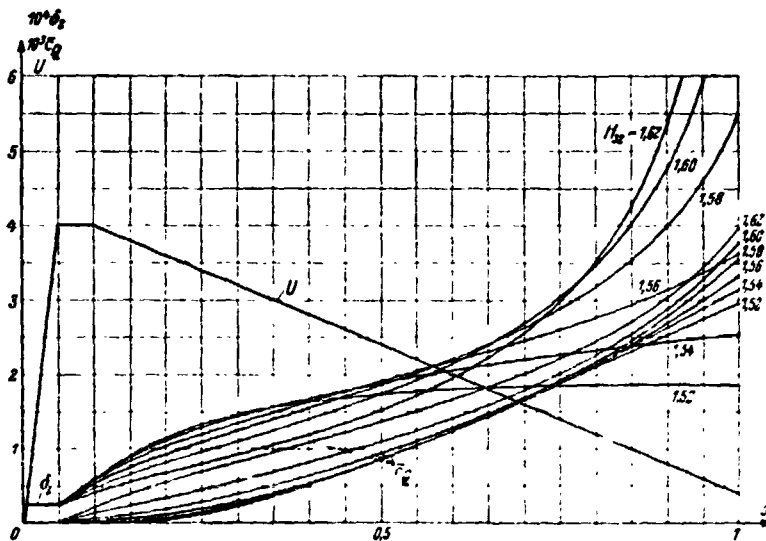

Fig. 13 Quantity Coefficient c_0 and Plus Loss Thickness δ_2 for Strong Pressure Increase and Form Parameter of the Laminar Boundary Layer, H_{32}, Being Constant; R = 2.10^6.

In Fig. 13, as well as in the following Figs. 14-16, the function

$$\bar{c}_Q = - \int_0^x v_0 dx \qquad (55)$$

46

is used throughout in place of v_0, in addition to δ_2 and H_{32}. This function offers a better overall picture than v_0 itself since the total amount of bleed-off is more important. At the trailing edge $\bar{c}_Q$ agrees with the often used quantity coefficient c_Q, before that $\bar{c}_Q$ provides the amount of bleed-off needed up to a point x while $-v_0$ is proportional to the slope of curve $\bar{c}_Q$.

A simple method for preventing separation is holding the form parameter constant through appropriate bleed-off. This bleed-off calculation can be carried out for laminar or turbulent cases by means of (54), setting b=0. At first the laminar boundary layer was calculated for various form factors, without consideration of instability and shift. The resulting values for δ_2 and $\bar{c}_Q$ are shown in Fig. 13. At first glance the result is surprising. One suspects at first that bleed-off to high H_{32} values should be much stronger and give correspondingly smaller values for δ_2. The calculation offers for x=1 values of $\bar{c}_Q$ that differ very little, while δ_2 is high for high H_{32} values and low for low ones, the exact opposite of what is expected offhand. Only at the start of the calculation does the picture correspond to expectation. As soon as this condition has become pronounced a smaller δ_2 occurs because of (54), in consequence (and because of the larger ϵ^*) a larger /243 $d\delta_2/dx$ with the increase in δ_2 predominating, so that the picture is quite reversed in the end. The reversal is easily recognized when (54) is entered into (36), b=0 and $H_{32}=\psi$. This results in

$$\frac{d\delta_2}{dx} = \frac{2D^* - \epsilon^*}{(H_{32} - 1)\,Re_{\delta_2}} - \left(3 - \frac{H_{12} - 1}{H_{32} - 1}\right)\delta_2\frac{1}{U}\frac{dU}{dx}. \qquad (56)$$

The first term, which is not dependent on $\delta_2 dU/dx$, actually gives a smaller $d\delta_2/dx$ with increasing H_{32} since the numerator

decreases and the denominator increases, according to Fig. 2.
The second term shows the opposite tendency. Since δ_2 is in
the denominator of the first term, but in the numerator of the
second one, the character of Fig. 13 is easily understood.
The second term predominates as soon as δ_2 has become larger.
Since δ_2 also goes into v_0 the lines for $\bar{c}_Q$ diverge later, but
much less so than those for δ_2.

During prevention of the separation the required amount
of bleed-off is predominant while δ_2 only goes into the resis-
tance (anyway quite high for high life coefficients). Ac-
cording to Fig. 13,the value of the form parameter,up to which
bleed-off takes place,does not have any big influence on the
amount of bleed-off.

That result is important because it shows that stability
of the laminar boundary layer, which increases strongly with
H_{32}, can be obtained even for strong increases of pressure
without a very large amount of bleed-off. This also confirms
another calculation where two pairs a,b, are entered into (54).
For case (A) a=1.40, b=0.02924,was chosen so that the region
below the strict shift condition in Fig. 8 not be exceeded,
while   case (B): a=1.37, b=0.02924,permits the region to
the upper straight line in Fig. 8, along which shift may al-
ready be expected. The results shown in Fig. 14 again demon-
strate very small differences for $\bar{c}_Q$, but bigger ones for H_{32}
and δ_2.

Particular attention is called to H_{32} having a maximum.
That points to a maximum of $Re\delta_2$, which is a function of the
strong increase of U. In case (B) even δ_2 has a maximum.
Since $-v_0$ also becomes very big, along with function $(1/U)dU/dx$
at around x=1, δ_2 does not continue to increase here any longer.
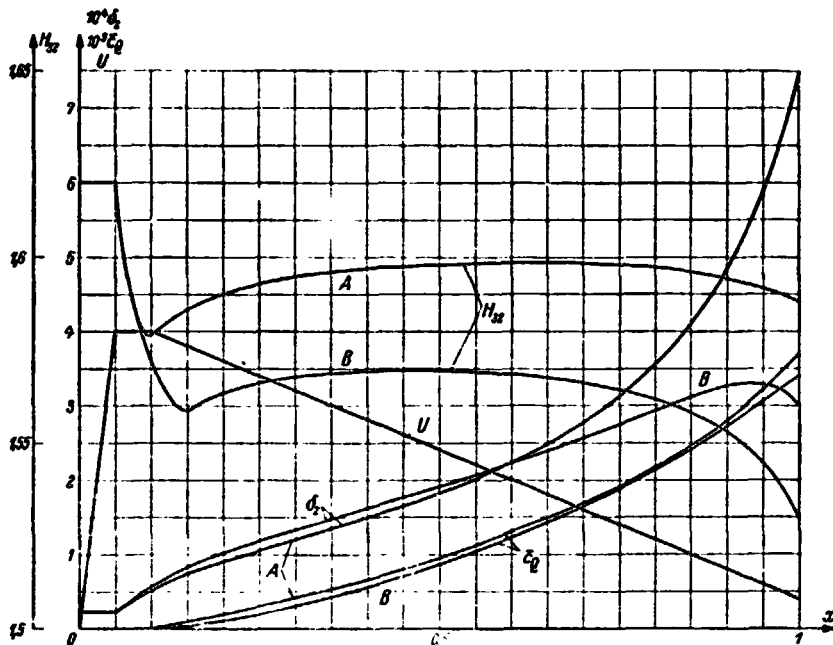
48

Fig. 14 Quantity Coefficient $\bar{c}_Q$, Form Parameter H_{32} and
Pulse Loss Thickness δ_2, for Strong Pressure Increase, Re =
2.10^6--(A) Bleedoff for Certain Prevention of Shift; (B) Pre-
vention of Shift no Longer Certain.

By putting (54) into (36) a closer picture can be obtained

here too.

f. Bleed-Off of the Turbulent Boundary Layer at Strong Pressure Increase

Since it is often not easy to maintain the boundary layer laminar with certainty, various attempts have been made recently to bleed-off the boundary layer so that no separation could occur [2]. To get some indication about how correct and rational such bleed-off is, some examples of turbulent boundary layers were calculated also for the velocity distribution of the previous examples.

/244

Here, too, it is again easiest to start calculating with constant form parameter. The resulting values for $\bar{c}_Q$ are shown in Fig. 15. Bleed-off starts a little later than for the laminar cases because there is a wait for the shift. Compared to the laminar cases the picture shows a complete shift. The $\bar{c}_Q$ lines show surprising overlapping. For smaller H_{32} values they seem to be more favorable. Later on the permitted increase of δ_2 during the initially small v_0 takes its toll with bleed-off amounts that can hardly be realized. The high values for H_{32} on the other hand are very high at the start with the required bleed-off. Even though bleed-off with a value of $H_{32}=1.95$ is most favorable in the end, the case appears unfavorable when compared to laminarity. The impression is gained therefore, at first, as if turbulent bleed-off is much less favorable. A series of additional calculation of samples shows, however, that the difference need not be so great. Apparently, bleed-off must be carried out with variable form paramter so that at first the values for H_{32} are small, increasing later on. For that reason (54) was used for the calculation and constants a,b set so that for,

50

$$\ln Re_{\delta_2} = 10(Re_{\delta_2} \approx 2000) \quad H_{32} = 1.95,$$

and for

$$\ln Re_{\delta_2} = 6(Re_{\delta_2} \approx 400) \quad H_{32} = 1.95 + k.$$

That results in

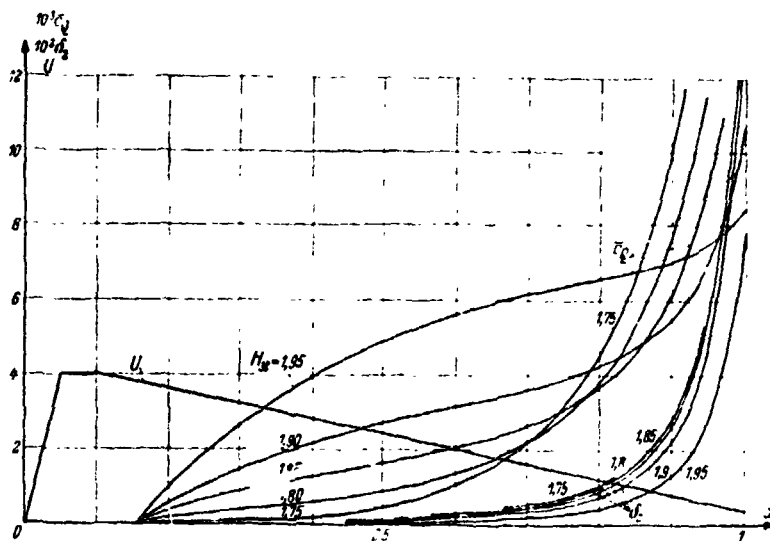$$a = 1.95 + 2.5 k \qquad b = -0.25 k. \tag{57}$$

Fig. 15 Quantity Coefficient $\bar{c}_Q$ and Pulse Loss Thickness δ_2 for Strong Pressure Increase and Constant Form Parameter H_{32} of the Turbulent Boundary Layer, Re = 2.10^6.

Since for higher values of k the form parameter attains high values close to 2, the calculation was carried out with a,b, calculated from (57) but only to $H_{32}=1.99$; above that a=1.99, b≈0,was used.

The results are shown in Fig. 16. It appears that values for $\bar{c}_Q$ have decreased significantly. It should be remembered that these calculations stop at values for H_{32} that are far

away from separation. Much more bleed-off than was necessary for prevention of separation took place then. By taking that into consideration and bleeding less off the trailing edge $\bar{c}_Q$ will perhaps not decrease exactly down to laminar values but it will be of the same order of magnitude.

The most favorable combination in Fig. 16, a=1.35, b=0.06, also turned out to be favorable for other cases where velocity is not linear. For the choice of a,b, in the turbulent case the total pressure increase is almost the only decisive indicator.

Values of c_Q obtained so far are of the same magnitude as those obtained experimentally by Raspet [2]. Unfortunately, no straightforward comparisons are possible since no experiments have been published so far for which distributions of pressure and bleed-off have been supplied. Another difficulty should be pointed out. The turbulent bleed-off calculations may in part lead to combinations of H_{32} and δ_2 where, according to estimates from section 4, the boundary layer thickness exceeds by far anything that is expected from the derivation of the boundary layer equations. Raspet and Cornish have pointed (unpublished) to experimental results that are not in agreement with the boundary layer equations. Understandably, δ_2 increases less in the experiment than in theory. On the one hand the theoretically available contribution F to δ_2, according to (30), cannot be determined experimentally from regions where the difference between u and U is very small, since potential flow can already be detected in such regions.

On the other hand the contributions of δ_2 that exceed a permissible boundary layer thickness reach into regions of potential flow where dU/dx is smaller than at the wall. It is

52

to be expected that the increase of δ_2, according to the pulse theorem, will not be reached, i.e., that the theoretical values for δ_2 and with it for v_0, are too large. That will keep one on the safe side for most problem situations.
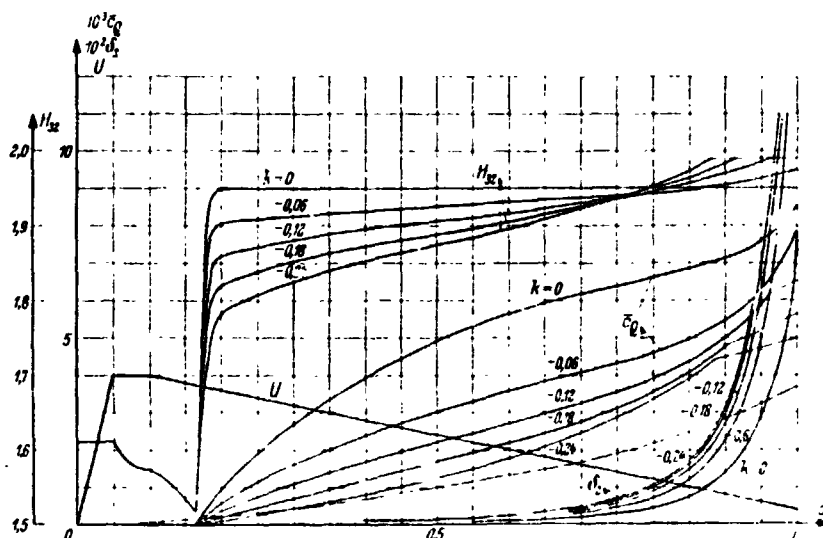

Fig. 16   Quantity Coefficient $\bar{c}_Q$, Pulse Loss Thickness δ_2, and Form Parameter H_{32} for Strong Pressure Increase and Bleed-Off of the Boundary Layer per (54) and (56), Re=2.10⁶. Dashed line: $\bar{c}_Q$ of case (A), Fig. 14.

Turbulent bleed-off is also to be considered as definitely positive for the high-lift case in general. The question which of the two types of bleed-off is preferable must be decided by practical considerations. Such a significant practical consideration would be that of safety.

Once a separation has taken place it can only be removed by a basic change in the pressure distribution, in all cases of bled off boundary layers. In the polar diagrams of air foils that produce a marked hysteresis both in the laminar and in the turbulent case. But judging from the line for the laminar $\bar{c}_Q$ in Fig. 16 that requires a little less bleed-off. But boundary layer shift alone can also lead to separation.

Since the high-lift case occurs primarily during takeoff and landing, where gnats, bugs and birds can force a boundary layer shift, it seems more appropriate here to apply turbulent bleed-off and even to monitor constantly whether laminar flow was not generated through oversight. In theory that can hardly happen since bleed-off comes too late for it. In practice bleed-off is more or less discontinuous so that the slight differences between laminar and turbulent siphoning are hard to verify at the start. It will probably be required to take precautionary measures not to work in a region where pure boundary layer shift alone can already cause separation and crash. It is possible that this may be the reason for two serious crashes that are so far unexplained.

REFERENCES

1. Schlichting, H. Grenzschicht-Theorie (Boundary Layer Theory), 3. edition. Karlsruhe, 1958.

2. Cornish, J. J. Practical High Lift Systems using distributed Boundary Layer Control, Res. Rep. 19, Aerophys. Dept. Miss. State Univ., 1958.

3. Kármán v., Th. Z. angew. Math. Mech. Vol. 1 (1921) p. 233.

4. Wieghardt, K. Ing.-Arch. 16(1948) p. 231.

5. Walz, A. Ing.-Arch. 16(1948) p. 243.

6. Wieghardt, K. Ing.-Arch. 22(1954) p. 368.

7. Truckenbrodt, E. Ing.-Arch. 20(1952) p. 211.

8. Ludwieg, H., and Tillmann, W. Ing.-Arch. 17(1949) p. 288.

9. Rotta, J. Ing.-Arch. 20(1952) p. 195.

10. Scholz, N. Ing.-Arch. 29(1960) p. 82.

11. Walz, A. Nouvelle méthode approché de calcul des couches limites laminaire et turbulente en écoulement compressible (A new approximation method for calculation of laminar and turbulent boundary layers in compressible flow). Publications scientifiques et techniques de Ministère de l'air, Paris, 1956.

12. Schlichting, H., and Pechau, W. Z. f. Flugwiss. 7(1959) p. 113.

13. Pechau, W. Jahrb. 1958 of WGL, p. 81.

14. Eppler, R. "Grenzschichtberechnung mit digitalen Rechenautomaten" (Calculation of boundary layers with automatic digital computers). Troisième Congrès Aéron. Europ. 1958, Tome II, p. 380 also Bericht MN 4 (Report MN 4) Bölkow-Entwicklungen KG.

15. Pohlhausen, K. Z. angew. Math. Mech. 1(1921) p. 252.

16. Wieghardt, K. "Zur turbulenten Reibungsschichte beim Druckanstieg" (The turbulent friction layer during pressure increase). Untersuchungen und Mitteilungen der deutschen Luftfahrtforschung (Transactions and communications of German aeronautical research), UM 6617 (1944).

17. Seyb, E. "Grenzschichtenrechnungen bei Druckanstieg" (Calculation of boundary layers during pressure increase). Report FM 120 of Bölkow-Entwicklungen, München 1961.

18. Unpublished communication to the author.

19. Seyb, E. "Näherungsweise Berechnung von Grenzschichten bei konstantem Energiedickenparameter H_{32}" (Calculation of boundary layers with constant form factor parameter H_{32}). Report MN 15 of Bölkow-Entwicklungen, KG, München 1961.

20. Eppler, E. <u>Z. f. Flugwiss.</u> 8(1960) p. 247.

21. Squire, H. B., and Young, A. D. "The calculation of the profile drag of airfoils," ARC-Report 1838 (1938).

22. Ulrich, A. "Theoretische Untersuchungen über die Widerstandsersparnis durch Laminarhaltung mit Absaugung" (Theoretical investigations of the saving in drag through maintenance of laminarity by bleeding). <u>Schriften d. dt. Akad. f. Luftforschung</u> I(1941) p. 58.

23. Pretsch, J. "Die Stabilität einer ebenen Laminarströmung by Druckgefälle und Druckanstieg" (Stability of a plane laminar flow for pressure increase and decrease). <u>Jb. d. dt. Luftforschung</u> I(1941) p. 58.

24. Schubauer, G. B., and Skramstad, H. K. "Laminar boundary layer oscillations and stability of laminar flow," <u>National Bureau of Standards Research Paper 1772</u> (reprint of secret NACA-Report of April 1943, later released as NACA Wartime Report W-8) and <u>J. Aer. Sci.</u> 14(1947) p. 69; also compare NACA-Report 909.

25. Granville, P. S. "The calculation of viscous drag of bodies of revolution." Navy Department, The David Taylir Model Basin, Report No. 849 (1953).

26. Raspet, A., and Györgyfalvy, D. <u>Schweizer Aero-Revue</u> 36 (1961) p. 151.

27. Howarth, L. <u>Proc. Roy. Soc.</u>, London, Series A 919, <u>164</u> (1938) p. 547.

28. Leigh, D. C. F. <u>Proc. Camb. Phil. Soc.</u> 51(1955) p. 320.

29. Wortmann, F. X. <u>Z. f. Flugwiss.</u> 5(1957) p. 228.

30. Iglisch, R. "Exakte Berechung der laminaren Reibungsschichte an der längsangeströmten ebenen Platte mit homogener Absaugung" (Rigorous Calculation of the laminar friction layer at the flat plate facing longitudinal flow, with homogeneous bleedoff), Schriften d. dt. Akad. d. Luftforschung 8B, No. 1(1944); NACA Techn. Memo. No. 1205 (1949).

31. Nickel, K. Ing.-Arch. 31(1962) p. 85.

2218. Eppler, R., Practical calculation of laminar and turbulent suction boundary layers (in German) Ingen.-Arch 32, s. 221-245. 1963.

The method is to use the momentum and energy integrals, making plausible assumptions about the dependence of the various terms on *u*, and δ, the momentum and energy thicknesses of the boundary layer. By this means two simultaneous, ordinary differential equations for δ₂, δ, are obtained which can be integrated numerically. Comparisons with a number of exact solutions are favorable.
                                                    K. Stewartson, England